



Mass of Saturn's magnetodisc: Cassini observations

C. S. Arridge,^{1,4} C. T. Russell,² K. K. Khurana,² N. Achilleos,¹ N. André,³ A. M. Rymer,⁵ M. K. Dougherty,¹ and A. J. Coates⁴

Received 28 November 2006; revised 26 January 2007; accepted 7 March 2007; published 12 May 2007.

[1] Saturn's ring current was observed by Pioneer 11 and the two Voyager spacecraft to extend 8–16 R_S in the equatorial plane and appeared to be driven by stress balance with the centrifugal force. We present Cassini observations that show thin current sheets on the dawn flank of Saturn's magnetosphere, symptomatic of the formation of a magnetodisc. We show that the centrifugal force is the dominant mechanical stress in these current sheets, which reinforces a magnetodisc interpretation – the formation of the current sheet is fundamentally rotational in origin. The stress balance calculation is also used to estimate the mass density in the disc, which show good agreement with independent in-situ measurements of the density. We estimate the total mass in the magnetodisc to be $\sim 10^6$ kg.

Citation: Arridge, C. S., C. T. Russell, K. K. Khurana, N. Achilleos, N. André, A. M. Rymer, M. K. Dougherty, and A. J. Coates (2007), Mass of Saturn's magnetodisc: Cassini observations, *Geophys. Res. Lett.*, 34, L09108, doi:10.1029/2006GL028921.

1. Introduction

[2] The presence of a substantial azimuthal current sheet in Saturn's magnetosphere was identified in Voyager and Pioneer magnetometer data and has been studied by a number of authors [e.g., *Giampieri and Dougherty*, 2004]. This current sheet is also clear in Cassini magnetometer data and modeling from Cassini's insertion orbit showed that the outer edge appeared to be much farther out than in the Pioneer/Voyager epoch [*Dougherty et al.*, 2005].

[3] It is of general interest to investigate the importance of various mechanical stresses – hot plasma pressure versus cold plasma centrifugal stresses – in accounting for the magnetic stress associated with the distorted magnetic field. From published Voyager magnetic field and particle data, *McNutt* [1984] made zeroth order estimates of the stress balance in Saturn's magnetosphere and concluded that the pressure gradient force was negligible beyond approximately 14 R_S . In a separate study, *Mauk et al.* [1985] reached essentially similar conclusions.

[4] In this paper we present observations from the magnetometer [*Dougherty et al.*, 2004] on the Cassini spacecraft

which show that Saturn's magnetospheric current sheet extends out to the magnetopause and distorts the field into a flattened disc of magnetic flux – Saturn's magnetodisc – similar to that in Jupiter's magnetosphere [e.g., *Smith et al.*, 1974]. We calculate the stress balance in this current sheet and find that the majority of the current is provided via stress balance with the centrifugal force, reinforcing the conclusions of *McNutt* [1984] and *Mauk et al.* [1985]. The inferred centrifugal force is used to calculate the mass density in the plasma sheet and we provide an order of magnitude estimate for the total mass in the magnetodisc.

2. Presence, Extent, and Dynamics of the Current Sheet

[5] Figure 1 shows fluxgate magnetometer data in cylindrical polar coordinates (B_r , B_ϕ , B_z) from Cassini's Rev 3 orbit of Saturn. The consistent radial field is evidence that significant azimuthal currents are present. Using a fairly simple axisymmetric current sheet model, the azimuthal currents have been modeled by a number of authors [e.g., *Giampieri and Dougherty*, 2004] and it has been shown that these currents extend 8–16 R_S in the equatorial plane. The B_r panel in Figure 1 clearly indicates that azimuthal currents extend right out to the magnetopause. This is in agreement with other observations made by Cassini which show the plasma sheet extending to the magnetopause [e.g., *Krupp et al.*, 2005].

[6] Based on the orientation and magnitude of the magnetic field we can divide the magnetosphere into three distinct regions: a strongly dipolar and almost curl-free region inside of 4 R_S , a quasi-dipolar region from 4 R_S to approximately 15 R_S , and a region with stretched magnetic field lines beyond 15 R_S at dawn. In the stretched region, the magnetic field lines are essentially radial forming a thin disc of magnetic flux analogous to the magnetodisc in Jupiter's magnetosphere.

[7] The magnetometer observations also reveal a very dynamic current sheet at dawn. Figure 2 shows 6 hours of fluxgate magnetometer data taken at a distance of $\sim 22 R_S$ on the dawn flank very close to the rotational equator. The radial field is consistently negative but undergoes transient decreases in magnitude approaching and occasionally passing through zero. This is evidence that the spacecraft has passed through the current sheet into the opposite magnetic hemisphere. These perturbations in B_r are usually associated with anti-phase perturbations in B_ϕ . We interpret these features as transient penetrations of the current sheet with a typical duration of 10–20 minutes. Such features were also evident in magnetometer data from Pioneer 11 [*Smith et al.*, 1980] and such current sheet encounters are observed in the terrestrial magnetotail [e.g., *Sergeev et al.*, 2004] and the Jovian magnetodisc [e.g., *Russell et al.*, 1999a].

¹Space and Atmospheric Physics Group, The Blackett Laboratory, Imperial College London, London, UK.

²Institute of Geophysics and Planetary Physics, University of California, Los Angeles, California, USA.

³Research and Scientific Support Department, European Space Agency, Noordwijk, Netherlands.

⁴Mullard Space Science Laboratory, University College London, London, UK.

⁵Applied Physics Laboratory, Johns Hopkins University, Laurel, Maryland, USA.

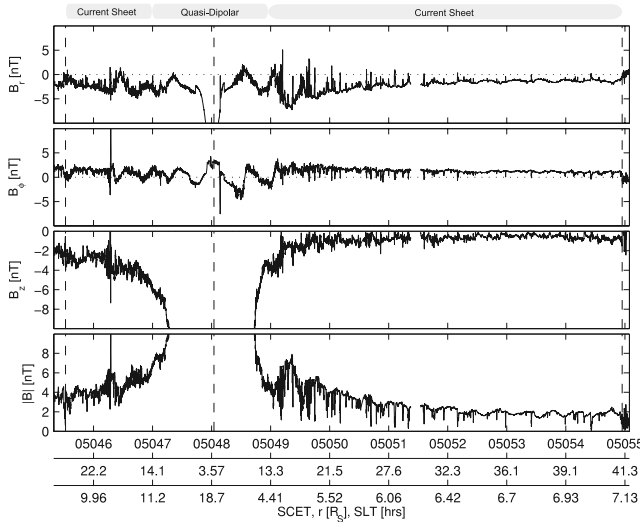


Figure 1. Cassini FGM data in body-fixed cylindrical polar coordinates, from the Rev 3 orbit of Cassini, showing a quasi-dipolar region and a current sheet region with radially stretched magnetic field lines.

[8] The detailed origin of these structures is beyond the scope of this paper, but we can use these transient crossings to examine the stress balance in the current sheet. The magnetometer data were surveyed for current sheet encounter signatures. In order to analyze the signatures most consistent with a current sheet encounter, the following objective criteria were used to select events for further analysis.

[9] Firstly, the radial field should reach zero through the event to ensure we reject partial crossings. These are not useful in the stress balance analysis since we require measurements at both the center and edge of the sheet. Secondly, there should be a clear anti-phase relation between B_r and B_ϕ throughout each event. Several effects might affect the accuracy of this linear polarization. Firstly, we estimate that magnetometer offsets may contribute ≈ 0.1 nT to the measured field. Secondly, there may be some additional field due to magnetopause currents. Thirdly, the current sheet may be quite distorted and so the coordinate system we use might not coincide with that of the current sheet. To account for these effects we allow B_ϕ to be several tenths of the lobe field B_ϕ when $B_r = 0$.

[10] Finally the event should be flanked by clearly defined lobe-type field. For our purposes this is defined as a steady field with B_r the dominant component and with low fluxes of electrons (as measured by the electron spectrometer on Cassini [Young et al., 2004]).

[11] From the examples in Figure 2 the encounters at 0050 and 0415 are included in the study, but the two other signatures do not meet our criteria. Both are partial crossings and the event near 0120 has a rather poor linear polarization.

3. Stress Balance

[12] The equations of stress balance in a thin current sheet were first developed for use at Jupiter by Vasylunas [1983]. In a rotating frame, neglecting gravity, differential rotation,

and Coriolis force effects, the time-stationary momentum equation can be written as:

$$\rho \mathbf{\Omega} \times (\mathbf{\Omega} \times \mathbf{r}) - \mathbf{j} \times \mathbf{B} + \nabla \cdot \mathbf{P} = 0 \quad (1)$$

where ρ is the mass density, $\mathbf{\Omega}$ is Saturn's angular velocity, \mathbf{j} is the current density, \mathbf{B} is the magnetic field, and \mathbf{P} is the pressure tensor. The magnetic field can be written as a superposition of Saturn's internal (dipolar) field and the field due to the current sheet. This allows us to cancel part of the magnetic stress since the dipole field is in stress balance with itself. In cylindrical polar coordinates and assuming that the pressure tensor is isotropic, and that $j_z B_\phi \ll j_\phi B_z$ (thin sheet approximation [Vasylunas, 1983]), the stress balance in the radial direction can be written as:

$$\rho \Omega^2 r = -\frac{B_z}{\mu_0} \frac{\partial B_r^{CS}}{\partial z} + \frac{\partial p}{\partial r} \quad (2)$$

[13] Here p is the scalar pressure, B_r^{CS} is the radial field due to the current sheet, and B_z is the total axial field. The magnetic pressure gradient term ($B_z \partial_r B_z^{CS}$) has been neglected since it is small at the center of the current sheet in comparison with the magnetic tension (curvature stress). The radial component of the curvature stress is formed by the vertical gradient of the current sheet radial field, $\partial_z B_r^{CS}$, and B_z .

[14] The first term on the right-hand side in equation (2) represents the curvature stress from the deformed field-lines wanting to straighten out and represents an inward force, the second term is the plasma pressure gradient force. The term on the left-hand side is the centrifugal force exerted on the plasma by the rotating configuration. The plasma pressure gradient and centrifugal forces are both outward forces.

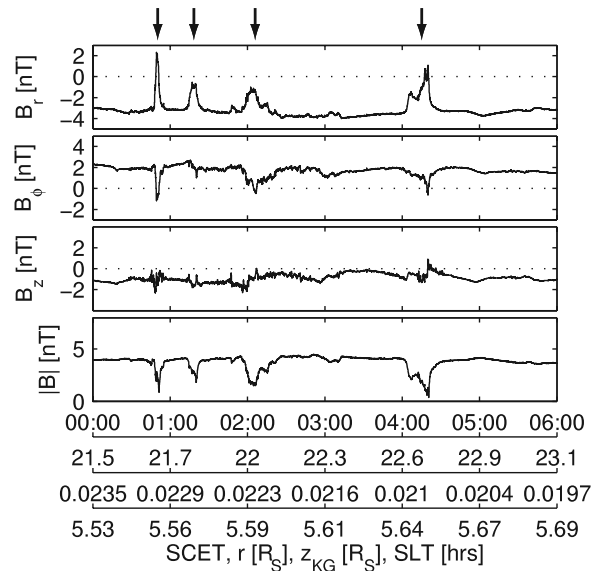


Figure 2. Examples of encounters with the current sheet, from the dawn flank on Cassini's Rev 3 orbit presented in cylindrical polar coordinates. This interval spans a radial range of 21.5–23.1 R_S and is at a constant $Z_{KG} \approx 0.02$ R_S northward of the rotational equator.

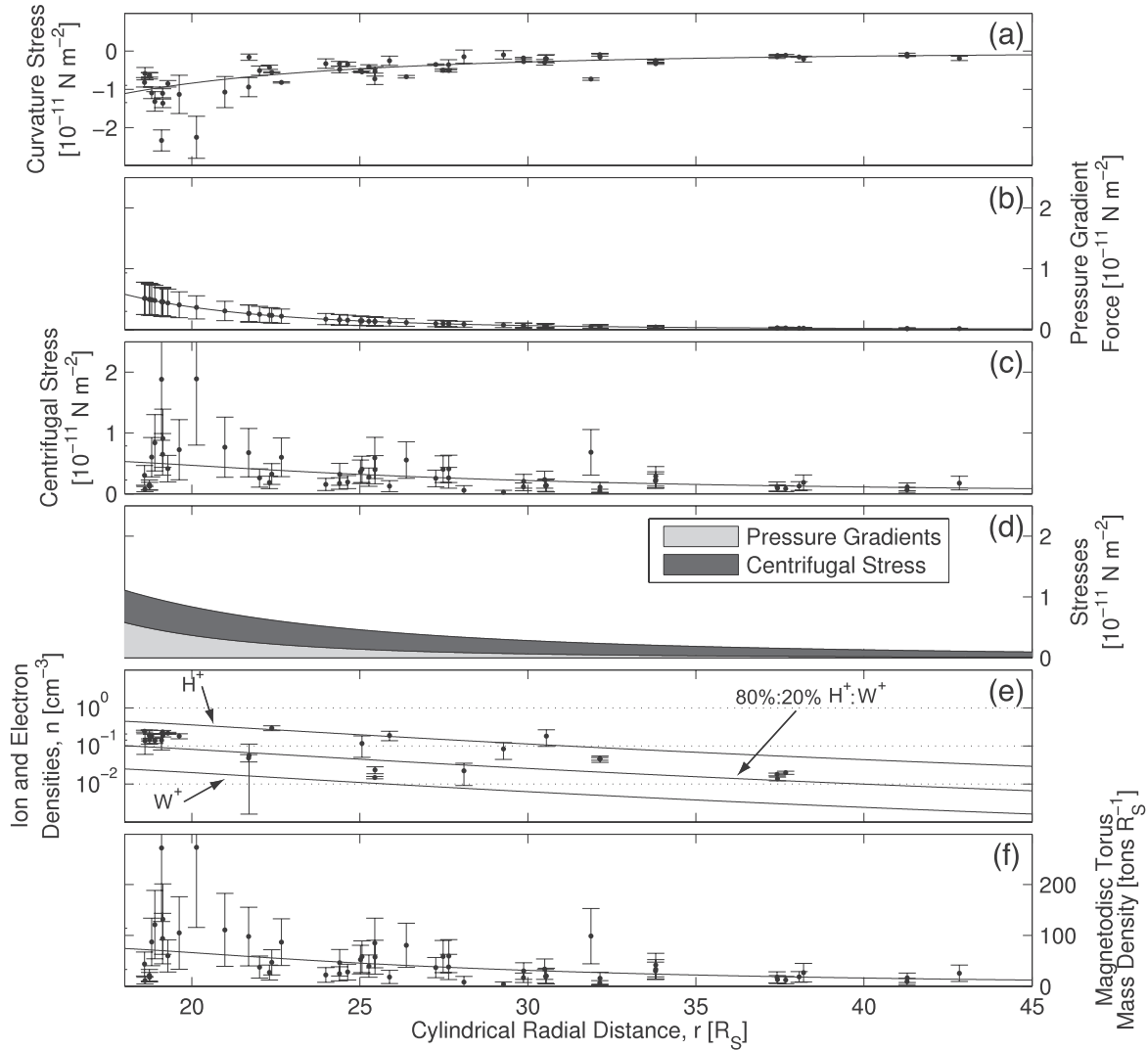


Figure 3. (a–f) Results of our stress balance calculations. Solid curves are the result of power-law fits to the data and indicate the average behavior in Figures 3a, 3b, 3c, 3e, and 3f. Figure 3d indicates the proportion of different mechanical stresses which balance the $\mathbf{j} \times \mathbf{B}$ force; these are determined using the power-law fits. The points with error bars in each panel are point measurements at each of our 58 current sheet encounters.

[15] By height-integrating equation (2) over the plasma sheet thickness of $2D$ the height-integrated magnetic curvature stress ($\int_{-D}^{+D} B_z \partial_z B_r^{CS} dz = -2B_z |B_r^{CS}(-D)|$) can be calculated directly from the magnetometer data. The radial field outside the current sheet, $B_r^{CS}(-D)$, and the total axial field B_z at the center of the current sheet, as determined when $B_r^{CS} = 0$, are determined directly from the magnetometer data at each current sheet encounter. Figure 3a shows the results of the calculation of the curvature stress. The error bars correspond to statistical uncertainties propagated from the measurements of $B_r^{CS}(-D)$ and B_z . The solid curve is the curvature stress calculated from $-2B_z |B_r^{CS}(-D)|$ using power-law fits to the measurements of $B_r^{CS}(-D)$ and B_z , and is given by: $-(3 \pm 1) \times 10^{-8} r^{(-2.7 \pm 0.3)}$.

[16] We can also use the magnetometer data to estimate the radial plasma pressure gradient force. Assuming pressure balance between the center of the plasma sheet and the lobes, the total (magnetic + plasma) pressure is constant across the sheet. Thus the radial gradient of magnetic

pressure in the lobes can act as a proxy for $\partial_r p$ at the center of the sheet.

[17] We have fitted a power-law to the total magnetic field strength in the lobes, as identified from quiet fields and low electron fluxes, and the magnetic pressure and its radial gradient then follow directly. The power-law for the radial magnetic pressure gradient force density is: $(1.2 \pm 0.5) \times 10^{-14} r^{(-4.3 \pm 0.1)}$. Since there is only one lobe field measurement inside of $18 R_S$, this power-law is subject to a bias and so we restrict our attention to the region beyond $18 R_S$.

[18] To be consistent with the height-integrated curvature stress we must integrate this magnetic pressure gradient force across the sheet. Applying simple current sheet models, the half-thickness of the current sheet has been found to lie between 1.5 and $3 R_S$ [e.g., *Giampieri and Dougherty, 2004*]. Thus we adopt a half-thickness of $2 R_S$ and integrate across the sheet assuming the stress is uniform. We also incorporate a factor of 0.5 to account for the (average) partition of the total pressure between the plasma

and the field over the width of the sheet. Figure 3b shows this height integrated plasma pressure gradient force. The uncertainties on this plasma pressure gradient force are calculated from the uncertainty in the fitted power-law parameters.

[19] The centrifugal stress can now be obtained from the assumption of stress balance, having calculated two of the three quantities in equation (2). The contributions of plasma pressure gradient and centrifugal stresses to balancing the total inward curvature stress are illustrated in Figure 3d. Beyond $20 R_S$ the centrifugal stress rapidly becomes dominant and the plasma pressure gradient force is negligible beyond $30 R_S$.

[20] The inferred centrifugal stresses allow us to calculate the mass density in the current sheet. The surface mass density σ can be calculated from the height-integrated centrifugal force $\sigma\Omega^2 r$. By dividing σ by the sheet thickness (again adopting a half-thickness of $2 R_S$) we obtain an average mass density which we can convert into an ion number density for different ion species.

[21] Since we do not accurately know the ion composition beyond $20 R_S$ we start by assuming either protons or water group ions are stressing the field. From this point of view, the proton and water group ion densities represent upper and lower limits on the calculated densities. Then we also calculate the ion density assuming a mix of protons (80%) and water group ions (20%) representing a 4:1 ratio by number density (1:4.5 by mass density assuming $m_{W^+} = 18 m_p$). These ion number density curves are plotted in Figure 3e.

[22] Given observations of plasma pressure gradient forces and curvature stresses, it is always possible to find a mass density which ensures stress balance, even if this implied mass density is negative! Whilst our mass densities are all positive, how do we know the calculated stress balance is accurate?

[23] Assuming that $n_e \approx n_i$ we compare electron number densities determined by the electron spectrometer on Cassini with the calculated ion number density curves. The electron densities lie between the proton and water group ion curves and this reasonable agreement shows that the calculated stress balance is accurate to at least an order of magnitude. The uncertainty of these number densities are the result of statistical averages over 1 minute intervals and the underlying physical uncertainties may be larger. At the present time such uncertainties have not been determined. Note that electron density measurements are not presently available for all the selected current sheet encounters due to data processing and data gaps.

[24] Figure 3f shows the result of further integrating the surface mass density in a torus around Saturn to calculate a linear mass density (per unit radial distance). Similar calculations at Jupiter [Russell *et al.*, 1999b] primarily investigated the region where the field distorts to form the magnetodisc whereas we discuss the region where the magnetodisc is more-or-less fully developed. Comparing measurements at the larger distance ranges in the study by Russell *et al.* [1999b, Figure 5], and the inner ranges presented in Figure 3f, the Jovian mass density ($\sim 10^4 \text{ tons } R_J^{-1}$) is around two orders of magnitude larger than the kronian value ($\sim 10^2 \text{ tons } R_S^{-1}$). We can integrate this curve between 18 and $45 R_S$ to estimate the total mass in the magnetodisc.

Evaluating this integral, we find a total magnetodisc mass of $\sim 10^6 \text{ kg}$ which we believe is at best an order of magnitude estimate because of the underlying uncertainties.

4. Discussion

[25] There is a reasonably good agreement between the power-law curves and the calculated quantities in Figure 3, however there is an enhancement in the magnetic stress near $20 R_S$. The outliers originate from two closely spaced current sheet encounters on two days, hence this may relate to spin-periodic features or time-dependent mass-loading. There is also the possibility that injection of mass from Titan near $20 R_S$ may require additional magnetic stress and so might be responsible for this enhancement.

[26] In our calculations we have assumed that the magnetospheric plasma is perfectly co-rotating. In principle one could take simultaneous measurements of the azimuthal flow velocity v_ϕ and accurately calculate the centrifugal stress through $\rho\Omega^2 r = \rho v_\phi^2 / r$. However such measurements are not routinely available and the only available model [Saur *et al.*, 2004] is limited to $r < 20 R_S$. At $20 R_S$ this model predicts a velocity which is $\approx 2/3$ of corotation. Hence there is a factor of at least 9/4 in the density estimations in Figures 3e–3f since a lower azimuthal velocity requires a larger mass density to achieve the same centrifugal force density.

[27] Pressure gradients in energetic particles are implicitly incorporated in our treatment of the plasma pressure gradient force, under the assumption of pressure balance across the plasma sheet. However we have explicitly ignored contributions due to pressure anisotropy in the force balance calculation. The fact that we find approximate force balance suggests that this may be negligible, at least in a gross global sense, but further work is required to confirm this.

[28] Our calculations have been carried out using measurements of transient current sheet crossings. The first implication of this is that the current sheet might be highly distorted, so our measurements of B_z at the center of the sheet might not accurately represent the field normal to the current sheet. The second implication is that such a distorted current sheet might be far from equilibrium. The density and stress profiles are relatively well ordered with radial distance which suggests this might be a second order effect. However, this might contribute to the apparent noise in our results. This noise might also be caused by other effects such as flux-tube interchange motions (locally changing the mass density on small-scales) or the neglect of radial acceleration in the momentum equation (which might not be valid locally, but should be a reasonable approximation in a gross global sense).

[29] We have demonstrated the presence of a significant magnetospheric current sheet in Saturn's magnetosphere. This current sheet extends out to the magnetopause and lies beyond the distance where models have traditionally placed the outer edge. The current sheet is dynamic and supports waves and/or flapping motions in response to internal or external perturbations. Via a stress balance analysis we have shown that the stretching of magnetic field lines beyond $20\text{--}30 R_S$ is caused primarily by the centrifugal force of the plasma sheet. We have used this analysis to calculate the

mass density in the plasma sheet, where the linear mass density is two orders of magnitude smaller than at Jupiter. We estimate the total mass in the magnetodisc to be $\sim 10^6$ kg. Our finding that the centrifugal stresses and plasma pressure gradient forces are essentially equal at $18 R_S$ is in good agreement with both McNutt [1984] and Mauk et al. [1985] who find a similar situation in their outer-most data-points at $\approx 15 R_S$ and $14 R_S$ respectively. However, further study of plasma pressure gradients is required to fully understand the stress balance in Saturn's magnetosphere.

[30] This stress balance analysis is evidence that this thin current sheet at dawn is a magnetodisc, and not attributed to magnetotail currents as was assumed from Pioneer 11 and Voyager 2 [Smith et al., 1980; Ness et al., 1982]. The formation of the magnetodisc is fundamentally rotational in origin.

[31] **Acknowledgments.** We would like to thank F. Crary, B. H. Mauk, H. J. McAndrews, C. Paranicas, E. C. Sittler, and M. F. Thomsen for useful discussions. CSA was supported in this work by a PPARC quota studentship and MKD by a PPARC senior fellowship. KKK and CTR were supported by NASA.

References

- Dougherty, M. K., et al. (2004), The Cassini magnetic field investigation, *Space Sci. Rev.*, *114*, 331–383.
- Dougherty, M. K., et al. (2005), Cassini magnetometer observations during Saturn orbit insertion, *Science*, *307*, 1266–1270.
- Giampieri, G., and M. K. Dougherty (2004), Modelling of the ring current in Saturn's magnetosphere, *Ann. Geophys.*, *22*(1), 653–659.
- Krupp, N., et al. (2005), The Saturnian plasma sheet as revealed by energetic particle measurements, *Geophys. Res. Lett.*, *32*, L20S03, doi:10.1029/2005GL022829.
- Mauk, B. H., S. M. Krimigis, and R. P. Lepping (1985), Particle and field stress balance within a planetary magnetosphere, *J. Geophys. Res.*, *90*, 8253–8264.
- McNutt, R. L. (1984), Force balance in outer planet magnetospheres, in *Physics of Space Plasmas, Proceedings of the 1982–4 MIT Symposia, SPI Conf. Proc. and Reprint Ser.*, vol. 5, edited by J. Belcher et al., pp. 179–210, Scientific, Gainesville, Fla.
- Ness, N. F., M. H. Acuna, K. W. Behannon, L. F. Burlaga, J. E. P. Connerney, R. P. Lepping, and F. M. Neubauer (1982), Magnetic field studies by Voyager 2: Preliminary results at Saturn, *Science*, *215*, 558–563.
- Russell, C. T., D. E. Huddleston, K. K. Khurana, and M. G. Kivelson (1999a), Structure of the Jovian magnetodisk current sheet: Initial Galileo observations, *Planet. Space Sci.*, *47*, 1101–1109.
- Russell, C. T., D. E. Huddleston, K. K. Khurana, and M. G. Kivelson (1999b), Observations at the inner edge of the Jovian current sheet: Evidence for a dynamic magnetosphere, *Planet. Space Sci.*, *47*, 521–527.
- Saur, J., B. H. Mauk, A. Kassner, and F. M. Neubauer (2004), A model for the azimuthal plasma velocity in Saturn's magnetosphere, *J. Geophys. Res.*, *109*, A05217, doi:10.1029/2003JA010207.
- Sergeev, V., A. Runov, W. Baumjohann, R. Nakamura, T. L. Zhang, A. Balogh, P. Louard, J. A. Sauvaud, and H. Rème (2004), Orientation and propagation of current sheet oscillations, *Geophys. Res. Lett.*, *31*, L05807, doi:10.1029/2003GL019346.
- Smith, E. J., L. Davis, D. E. Jones, P. J. Coleman, D. S. Colburn, P. Pyl, C. P. Sonett, and A. M. A. Frandsen (1974), The planetary magnetic field and magnetosphere of Jupiter: Pioneer 10, *J. Geophys. Res.*, *79*, 3501–3513.
- Smith, E. J., L. Davis, D. E. Jones, P. J. Coleman, D. S. Colburn, P. Dyal, and C. P. Sonett (1980), Saturn's Magnetosphere and its interaction with the solar wind, *J. Geophys. Res.*, *85*, 5655–5674.
- Vasyliunas, V. M. (1983), Plasma distribution and flow, in *Physics of the Jovian Magnetosphere*, edited by A. Dessler, chap. 11, pp. 395–453, Cambridge Univ. Press, New York.
- Young, D. T., et al. (2004), Cassini plasma spectrometer investigation, *Space Sci. Rev.*, *114*, 1–112.
- N. Achilleos, C. S. Arridge, and M. K. Dougherty, Space and Atmospheric Physics Group, Blackett Laboratory, Imperial College London, London SW7 2BW, UK. (chris.arridge@physics.org)
- N. André, Research and Scientific Support Department, European Space Agency, Keplerlaan 1, Noordwijk NL-2200 AG, Netherlands.
- A. J. Coates, Mullard Space Science Laboratory, University College London, London RH5 6NT, UK.
- K. K. Khurana and C. T. Russell, Institute of Geophysics and Planetary Physics, University of California, Los Angeles, CA 90095, USA.
- A. M. Rymer, Applied Physics Laboratory, Johns Hopkins University, Laurel, MD 20723, USA.